Old stars in young clusters: Lithium depleted low-mass stars of the Orion Nebula Cluster[1]

F. Palla[1], S. Randich[1], Ya. V. Pavlenko[2], E. Flaccomio[3], R. Pallavicini[3]

ABSTRACT

We measured lithium in a sample of low-mass stars ($\sim$0.1-0.3 $M_\odot$) of the Orion Nebula Cluster. We find evidence for significant Li depletion in four high probability members, corresponding to nuclear ages between $\sim$15 and 30 Myr. In two cases, there is excellent agreement between the mass and age based on models of Li burning and those derived from the HR diagram, reinforcing our early findings (Palla et al. 2005). For the two other stars, the nuclear age is significantly larger than the isochronal one. Several Li-depleted stars display accretion activity, veiling and emission lines. We discuss empirical evidence in favor of the old nuclear age and the implications on the star formation history of the Orion cluster.

Subject headings: Stars: formation - Stars: pre-main sequence - Stars: abundances - Open clusters and associations: individual (Orion Nebula Cluster)

1. Introduction

Exploiting the rich low-mass population of the Orion Nebula Cluster (ONC), we have found two bona-fide members showing a significant amount of Li depletion that imply nuclear ages of about 10-12 Myr for stars with mass $\sim$0.4 $M_\odot$, consistent with the isochronal ages (Palla et al. 2005, Paper I). This result is surprising in view of the expected youth of the ONC, whose bulk population is only 1-2 Myr old (Hillenbrand 1997, hereafter H97). The identification of these ONC stars has important implications on theories of cluster formation and evolution that envisage a rather extended phase of stellar production, in addition to a

---

[1]INAF–Osservatorio Astrofisico di Arcetri, L.go E. Fermi, 5, I-50125 Firenze, Italy palla@arcetri.astro.it

[2]Main Astronomical Observatory, Academy of Sciences, Golosiiv Woods, Kiev-127, 03680 Ukraine

[3]INAF–Osservatorio Astronomico di Palermo, Piazza del Parlamento 1, I-90134 Palermo, Italy

[1]Based on data collected at ESO-VLT, Paranal Observatory, Chile (ID 074.C-0757(A))

short-lived activity when the bulk of the population is assembled. Interestingly, the ONC does not seem to be an exceptional case, since Li-depleted stars have been found in other young systems such as Upper Scorpius (Martín 1998) and σ Orionis (Sacco et al. 2007).

Measurements of the surface Li abundance in fully convective low-mass stars ($M_* \lesssim 0.5\,M_\odot$) in young clusters provide a critical test to stellar evolution models as well as a useful clock to estimate nuclear ages that can be compared to the isochronal ages derived from the star's location in the HR diagram (e.g., Jeffries 2006). The latter, however, are subject to a variety of systematic uncertainties related to poorly known stellar (spectral types, luminosities, multiplicity) and cluster (distance, extinction) properties. On the contrary, Li abundance determinations can result in more accurate age estimates (e.g., Bildsten et al. 1997).

In this Letter, we present new Li observations of a sample of ONC stars that extends the mass interval of Paper I close to the substellar limit. The stars have been selected from the optical catalog of H97 on the basis of their spectral types (from M1 to M4) and high membership probability ($\gtrsim$90%) from proper motion studies. Their location in the HR diagram is shown in Figure 1, along with the predicted region of Li burning and depletion.

2. Observations and data reduction

The observations were carried out in Service mode on October 19 and November 12/14/24 2005 using FLAMES (Pasquini et al. 2000) mounted on VLT-Kueyen (UT2). The Giraffe spectrograph and Medusa fiber system were used in conjunction with the 316 lines/mm grating and order sorting filter 15 yielding a nominal resolving power R=19,300 and a spectral coverage from 660.7 to 696.5 nm that includes the He I 667.8 nm and Li I 670.8 nm lines. Two fiber configurations were observed in four separate 45 min. exposures, centered at RA(2000)=05h 35m 00.0s and DEC(2000)=−05d 23m 10s and RA(2000)=05h 35m 36.0s and DEC(2000)=−05d 18 00s. MEDUSA fibers were allocated to 102 and 58 targets in the two configurations, with 21 stars in common. In total, we obtained spectra of 139 stars, 57 of which with spectral type later than M1 that are the object of the present study.

Data reduction was carried out using the Giraffe BLDRS pipeline, following the standard steps. Sky contribution was separately subtracted employing the same method described in Paper I. We determined radial velocities for all stars using the BLDRS software, while pseudo-equivalent widths (pEWs) of the Li I 670.8 nm doublet were measured using MIDAS by direct integration with respect to the pseudo-continuum formed by the haze of molecular lines over a region of $\sim$ 0.2 nm around the Li line (Pavlenko 1997). When present in emission, we also measured the pEW of the He I 667.8 nm line which is recognized as an accretion diagnostic in young low-mass stars (e.g., Mohanty et al. 2005).

3. Derived lithium abundances

The majority of our sample stars are affected by spectral veiling, which needs to be taken into account before determining Li abundances from measured pEWs. We determined the veiling value r from the measurements of the pEWs of three strong lines (Ni I 664.3 nm, Fe I 666.3 nm, V I 662.5 nm) in our spectra and in those of unveiled stars of similar temperature belonging to the older clusters IC 2602 and IC 2391 (cf. Paper I). The ratio of the pEWs of the IC 2602/IC 2391 and ONC stars gives $1 + r$. We assumed as final value of r the average of the three lines. For a few highly veiled and/or very cool stars we compared the spectrum of the veiled star with that of a star of the same temperature unaffected by veiling to which we progressively added continuum flux to mimic veiling until a good match between the two spectra was obtained. Resulting veiling values vary in the range $r \sim 0 - 9$ with a median $r = 2.8$ (75th percentile=1.7). A correlation between near-infrared (NIR) excess and/or He I pEWs and the veiling r is present, as expected.

Abundances were determined from pEWs using new curves of growth (COGs) generated from a grid of synthetic spectra in the wavelength range 669.0-673.0 nm using the WITA6 code (Pavlenko 2000) and NextGen model atmospheres (Hauschildt et al. 1999). Synthetic spectra were obtained with a step of 0.0025 nm in wavelength and were then convolved with the appropriate gaussian profile to match the resolution of our observed spectra ($\Delta\lambda \simeq$ 0.035 nm). We have produced a grid of theoretical spectra considering eight values of Li abundances (A(Li)=0, 0.5,..3.5, where A(Li)=log N(Li)/N(H)+12), six values of $T_{\rm eff}$ (3100, 3200,..3600 K), and two values of surface gravity (log g=4.0, 4.5) in order to cover the parameter space of our sample stars. Predicted pEWs were measured in the synthetic spectra considering the same spectral range as for the observed spectra. Corresponding COGs are listed in Table 1. Note the non-monotonic trend of the COGs as a function of $T_{\rm eff}$ which is due to the relative contribution of TiO bands and lithium. Li abundances were then derived by interpolating between COGs. For the four stars discussed in Paper I, the new abundances are a factor ∼1.3–2.6 higher than those obtained using MOOG (Sneden 1973) and Kurucz (1993) model atmospheres. As a result, only two of them have A(Li) still significantly below the interstellar value. The reason for this change is related to the use of more appropriate model atmospheres and an improved treatment of the contribution of molecular bands (mainly TiO) in the 670.8 nm spectral region. Random errors in derived abundances are due to uncertainties in stellar parameters, pEWs, and veiling. Specifically, conservative errors of 150 K in Teff, 0.5 dex in log g, 10-20% in pEW reflect into Li abundance uncertainties of ∼0.1, 0.2, and 0.2-0.4 dex, respectively. Adding them in quadrature, the total error in A(Li) is ∼0.3-0.5 dex.

The resulting Li abundances of the new sample vary between A(Li)=2.9–4, and in most cases are consistent with the interstellar value (A(Li)=3.1–3.3). However, four stars show an amount of Li depletion ∼ 5–60, larger than that found in Paper I. In order to check whether the low values of Li abundances of these stars could be due to incorrect determination of r (see Table 3 for the numerical values), we compared their spectra to those of Li undepleted stars of similar spectral type unaffected by veiling and artificially veiled by the amount derived from the three lines. The comparison is displayed in Figure 2: the dotted line is the observed line in 3 ONC stars with no veiling and the dashed line is what that star's spectrum would look like with the veiling that was found for the Li-depleted star. A good agreement is reached for all the spectral features, apart from the Li line that remains much weaker in the Li depleted stars.

4. Nuclear and isochronal ages

The position in the HR diagram of the four stars with low Li abundance is marked in Figure 1, along with those of Paper I. The mass and age of each star, derived using Palla & Stahler (1999; hereafter PS99), are listed in Table 2, where the associated error has been computed assuming an uncertainty of ±150 K in temperature and ±0.2 dex in luminosity. Stellar masses vary between ∼0.1 and 0.3 $M_\odot$ and isochronal ages between ∼2 and 28 Myr. Comparison with models by D'Antona & Mazzitelli (1998), Baraffe et al. (1998), and Siess et al. (2000) yields similar values (to within 20% in mass and up to a factor of 2 in age).

As in Paper I, we utilize the relations for the time variation of luminosity and Li-depletion derived by Bildsten et al. (1997) for fully convective objects undergoing gravitational contraction. The location of the six depleted stars in the plot of the mass-depletion time relation is shown in Figure 3. The derived values of mass and age are listed in the last two columns of Table 2. As is evident from Fig. 3, stars #770 and 525 have nuclear and HR mass and age estimates that agree to within 10%, similar to what found for stars #775 and 3087 using the revised Li abundances (see Table 2). This result confirms the usefulness of Li to test PMS models down to ∼0.2 $M_\odot$ and ages up to ∼25 Myr.

On the other hand, the analysis on stars #307 and 327 gives very discrepant values for both mass and age: while the HR diagram indicates a mass of ∼0.1-0.2 $M_\odot$ and age of 2-3 Myr, the large amount of Li depletion can only be explained by more massive (∼0.5 $M_\odot$) and older (15-20 Myr) stars. In other words, these two stars have experienced too much burning for the estimated ages. In order to reconcile the two estimates, the luminosity should be decreased by a factor of 7-10 and/or the effective temperature increased by several × 100 K, a rather extreme change that could be accounted for by a combination of effects (binarity, photometric variability, incorrect spectral type assignment). Conversely, an increase of the Li abundance of these two stars up to the interstellar value would require a pEW higher by a factor of ∼2, much larger than the combined uncertainty on pEW measurement and r (see previous section). We also note that NLTE effects, and in particular Li overionization due to the heating of accreting matter, might decrease the strength of the Li line. However, we do not find a correlation between veiling-corrected pEWs and r-values, as one would expect if pEWs were affected by accretion. Finally, several stars that appear old from the position in the HR diagram have Li abundances consistent with the interstellar value, suggesting that their parameters (L, $T_{\rm eff}$) are likely incorrect.

The six Li-depleted stars have membership probability from proper motion equal to 99%, and radial velocities (see Table 3) in good agreement with that of the ONC ($V_r \simeq 26.5 \pm 2.3$ km s^{-1}, Sicilia-Aguilar et al. 2005), except #525 that shows a variable velocity, and #307 and #775 with $V_{\rm r}$ slightly different from the cluster average, but still consistent within the errors (random and systematic). Also, they are located in the innermost region of the ONC cluster, supporting the assumption that they represent bona fide members and not a contamination from the nearby older Orion Ib association.

Table 3 also lists some useful quantities derived from our spectral analysis, including information on veiling, presence of He I 667.8 nm line emission, together with NIR excess and X-ray properties. Star #770 with consistent values of $t_{\rm Li}$ and $t_{\rm HRD}$ (∼20 Myr) has a large NIR excess and He I line emission. Also, star #3087 with elevated X-ray luminosity is a proplyd candidate (239-510) without silhouette disk or jet/microjet and has NIR colors of classical T Tauri stars (O'Dell & Wong 1996, Kastner et al. 2005). Finally, the two stars (#307, 327) with discrepant $t_{\rm Li}$ and $t_{\rm HRD}$ have most indicators consistent with the old age estimate, and #327 has not been detected in X-rays (Getman et al. 2005). Thus, while there is no obvious systematic trend, the presence of youth indicators suggests that these phenomena may survive for long times in very low-mass stars.

5. Discussion

The Li-test on a large sample of the optically visible, low-mass ONC stars has revealed the presence of a small group of bona fide members with Li abundances well below the interstellar value. The time scale required to reach the measured depletion levels varies between several Myr and about 30 Myr. In most cases this nuclear age is in excellent agreement with the isochronal age. Thus, there is independent evidence for a population of old stars mixed with the much larger assembly of young objects that formed in the last 1-2 Myr and that, correspondingly, do not exhibit Li depletion.

The concept of large age spreads in young clusters and associations based on isochronal ages has been criticized arguing that the initial time for contraction is not necessarily the birthline computed with a fiducial value of the protostellar accretion rate (10^{-5} M$_\odot$ yr^{-1}, PS99), but from a variety of birthlines, each corresponding to a different accretion history (e.g., Hartmann 2003). Thus, the location of a given star in the lower portion of the HR diagram can also be interpreted as the end of the main accretion phase without significant PMS contraction. Consequently, for the faintest low-mass ONC stars there exists the possibility that, owing to the small radii and elevated central temperatures, they might have experienced Li-burning during the protostellar phase. What would then be the typical accretion rate such that the central value of the temperature equals the critical value for Li-ignition, $T_{\rm Li} = 3 \times 10^6$ K? For simplicity, assuming a fully convective interior, the polytropic relation for the central temperature is: $T_{\rm c} = 7.5 \times 10^6$ K $(M_{\rm p}/1M_\odot)(R_{\rm p}/1R_\odot)^{-1}$ (Stahler & Palla 2004, eq. 16.37). Thus, requiring $T_{\rm c} = T_{\rm Li}$ for a 0.1-0.2 M$_\odot$ protostar, implies a radius of $\sim$ 0.3-0.5 R$_\odot$. Such small structures can only be achieved if the mass accretion rate is greatly reduced from the fiducial one, below 10^{-7} M$_\odot$ yr^{-1} (Stahler 1988). This would imply a very long accretion phase, at least several Myr for the formation of a 0.2 M$_\odot$ protostar. Moreover, the depletion time scale to reach the measured Li abundances in the ONC stars would still be significantly larger than the accretion time. Therefore, we conclude that the correction for a lack of a contraction phase prior to Li burning is not significant for the ONC Li-depleted stars and that in any case Li burning in the protostellar phase would imply long accretion times, contrary to the idea of fast stellar formation. Finally, even modest but measurable levels of Li depletion require time scales longer than few Myr.

We may ask why there are apparently only few old stars in the ONC. In our view, part of the reason reflects the property that star formation in clusters begins at low levels and then picks up at a fast rising rate (e.g. Palla & Stahler 2000). In addition, there is a selection effect in the optically selected survey by H97 which is complete only to a luminosity $L_* \gtrsim 0.1$ L$_\odot$. This limit corresponds to an age of 10 Myr for a 0.4 M$_\odot$ star and to $\sim$3 Myr for a 0.2 M$_\odot$ star, thus explaining the inhomogeneous distribution in the HR diagram (see Fig. 1) and the scarcity of faint objects. The incompleteness gives the impression that lower-mass stars tend to be younger than their higher mass counterparts, as also noted in other SFRs (e.g., Hartmann 2003). However, Huff & Stahler (2006) have shown that there is no age-mass correlation in the complete sample of ONC stars with mass $\gtrsim 0.4$ M$_\odot$. Thus, it is entirely plausible that there exists a larger population of previously unnoticed faint and old very low-mass stars. The fact that Slesnick et al. (2004) have identified a group of old stars (isochronal ages), selected from infrared observations, reinforces this view.

In conclusion, the combination of Li measurements and deeper spectroscopic observations of the more embedded stars are providing a picture of the history of ONC that cast doubts on models of rapid star formation and strengthens the empirical finding of a time dependent pattern of star births. Observationally, the next challenge will be to obtain independent estimates of the ages of stars intermediate between the dominant young population ($\lesssim$ 1-2 Myr) and the evolved one ($\gtrsim$ 10-30 Myr) probed by the Li test. Theoretically, realistic physical models of cluster-forming clouds must be constructed allowing for a prolonged stellar birth activity, albeit at different rates.

REFERENCES

Baraffe, I., Chabrier, G., Allard, F., & Hauschildt, P.H. 1998, A&A, 337, 403

Bildsten, L., Brown, E.F., Matzner, C.D., & Ushomirsky, G. 1997, ApJ, 482, 442

D'Antona, F., & Mazzitelli, I. 1998, ASP Conf. Ser. 134, eds. R. Rebolo et al., 442

Getman, K.V., Flaccomio, E., Broos, P.S. et al. 2005, ApJS, 160, 319

Hartmann, L. 2003, ApJ, 585, 398

Hillenbrand, L.A 1997, AJ, 113, 1733 (H97)

Hillenbrand, L.A & Carpenter, J.M. 2000, ApJ, 540, 236

Huff, E.M., & Stahler, S.W. 2006, ApJ, 644, 355

Jeffries, R.D. 2006, in Chemical Abundances and Mixing in Stars, eds. S. Randich & L. Pasquini (Springer-Verlag), p. 68

Kastner, J.H., Franz, G., Grosso, N., et al. 2005, ApJS, 160, 511

Kurucz, R.L. 1993, CD-ROM 13, ATLAS9 (Cambridge: SAO)

Martín, E.L. 1998, AJ, 115, 351

Mohanty, S., Jayawardhana, R., Basri, G. 2005, ApJ, 626, 498

O'Dell, C.R., Wong, K. 1996, AJ, 111, 186

Palla, F., & Stahler, S.W. 1999, ApJ, 525, 772 (PS99)

Palla, F., & Stahler, S.W. 2000, ApJ, 540, 255

Palla, F., Randich, S., Flaccomio, E., Pallavicini, R. 2005, ApJ, 626, L49

Pasquini, L., Avila, G., Allaert, E. et al. 2000, SPIE, 4008, 129

Pavlenko, Ya. 2000, Astron. Rept., 45, 144

Sacco, G.G., Randich, S., Franciosini, E., Pallavicini, R., Palla, F. 2007, A&A, 462, L23

Sicilia-Aguilar, A., Hartmann, L.W., Szentgyorgyi. A.H., et al. 2005, AJ, 129, 363

Siess, L., Dufour, E., Forestini, M. 2000, A&A, 358, 593

Slesnick, C.L., Hillenbrand, L.A., & Carpenter, J.M. 2004, ApJ, 610, 1045

Sneden, C. 1973, ApJ, 184, 839

Stahler, S.W. 1988, ApJ, 332, 804

Stahler, S.W., Palla, F. 2004, The Formation of Stars (Wiley-VCH)

This preprint was prepared with the AAS LaTeX macros v5.2.

Table 1: Curves of growth of theoretical pEWs (in mÅ) of the Li I 670.8 nm line. For each temperature, the two pEWs correspond to log g =4.0 and 4.5.

A(Li)	$T_{\rm eff}$ (K)					
	3100	3200	3300	3400	3500	3600
0.0	148/159	141/150	137/147	140/150	150/155	156/169
0.5	190/207	182/199	178/192	176/191	182/194	192/209
1.0	259/281	249/271	241/260	234/257	237/255	241/273
1.5	341/362	329/350	317/341	305/331	298/328	303/340
2.0	417/437	406/423	385/410	370/399	360/392	358/404
2.5	483/505	470/490	452/476	426/457	415/450	411/462
3.0	550/562	533/549	510/533	484/514	466/505	463/513
3.5	598/620	586/606	562/583	536/571	523/559	520/576

Table 2. Properties of the Li-depleted stars found here (first four) and in Paper I. ID designation is from Hillenbrand (1997). Stellar parameters are from Getman et al. (2005).

ID	log L ($L_\odot$)	log T_{eff} (K)	ST	pEW (mÅ)	A(Li)	M_{HRD} ($M_\odot$)	t_{HRD} (Myr)	M_{Li} ($M_\odot$)	t_{Li} (Myr)
307	−1.11	3.513	M3	300	1.3±0.4	0.18±0.04	2.6±0.9	0.49±0.06	15.9±1.9
327	−1.21	3.491	M4	390	1.8±0.5	0.12±0.04	1.9±0.9	0.47±0.06	18.9±1.9
525	−1.77	3.513	M3e	395	1.9±0.3	0.19±0.04	28.4±9	0.21±0.02	28.2±5.0
770	−1.46	3.535	M2.5	435	2.4±0.3	0.29±0.04	21.5±9	0.28±0.03	18.2±2.0
775	−1.01	3.557	M1	471	2.8±0.4	0.39±0.07	9.7±3.9	0.42±0.07	$10.2^{+1.6}_{-2.5}$
3087	−1.01	3.557	M1	421	2.4±0.4	0.39±0.07	9.8±3.8	0.44±0.07	10.9±1.7

Table 3. Membership & Youth Indicators

ID	V_r^a (km s^{-1})	$r^a_{1,2,3}$	He I^a (Å)	NIR^b	log L_X^c (erg s^{-1})
307	21.0±2.6	0.4, –, 0.7	abs.	0.18	28.95
327	24.2±2.9	1.9,1.3,–	23.7	0.77	u.l.
525	var.	0.5,0.07,0.4	abs.	—	28.45
770	25.9 ±1.8	2.8, 2.6, –	16.5	2.65	29.79
775	31.6±3.2	5.0	14.8	—	29.20
3087	27.5±4.0	4.5	13.6	1.81	29.70

[a] V_r, r, He I: this paper. r values from 3 different lines.

[b] NIR excess: from Hillenbrand & Carpenter (2000)

[c] L_X: from Getman et al. (2005)

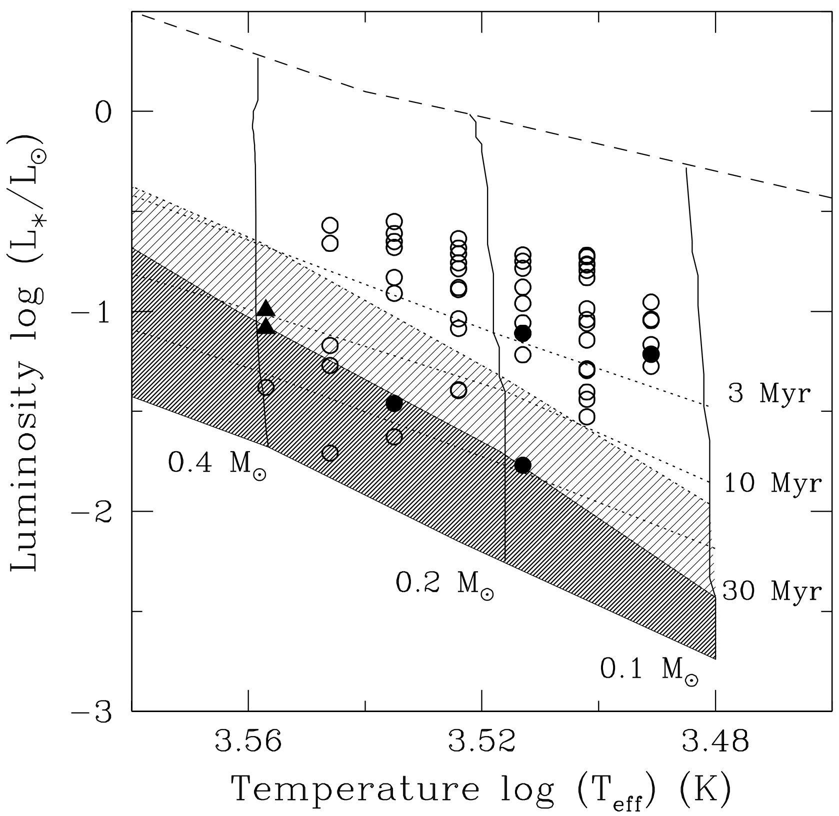

Fig. 1.— The distribution in the HR diagram of the observed 57 stars. The hatched regions indicate different levels of predicted Li depletion: up to a factor of ten (light grey) and more (dark grey) below the initial value according to the models of Siess et al. (2000). Selected masses and isochrones from PS99 are indicated. Filled symbols are the depleted stars from this study (circles) and Paper I (triangles).

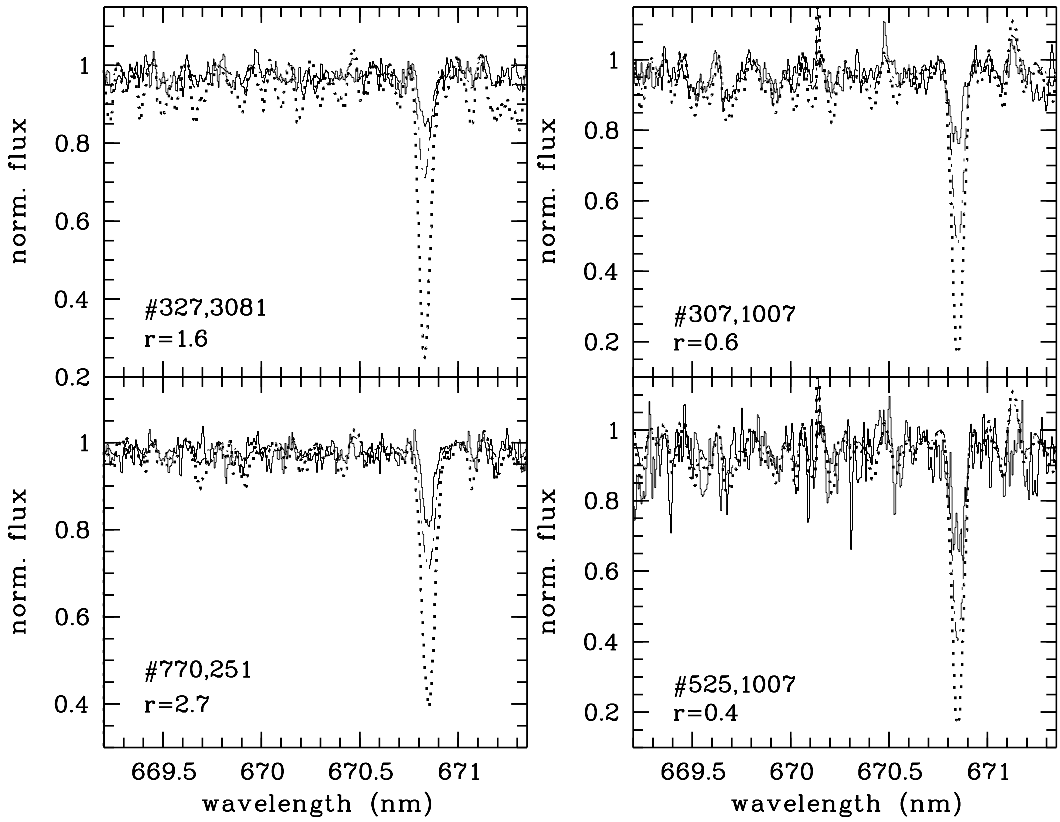

Fig. 2.— Spectra in the Li line region of the four depleted stars (#307, 327, 525, 770; solid lines). In each panel, the dashed lines show the spectra of three ONC stars (#251,1007,3081) with the same spectral type unaffected by veiling, while the long-dashed lines are the artificially veiled spectra by the amount r, as labeled. S/N ratios are in the range 35–60.

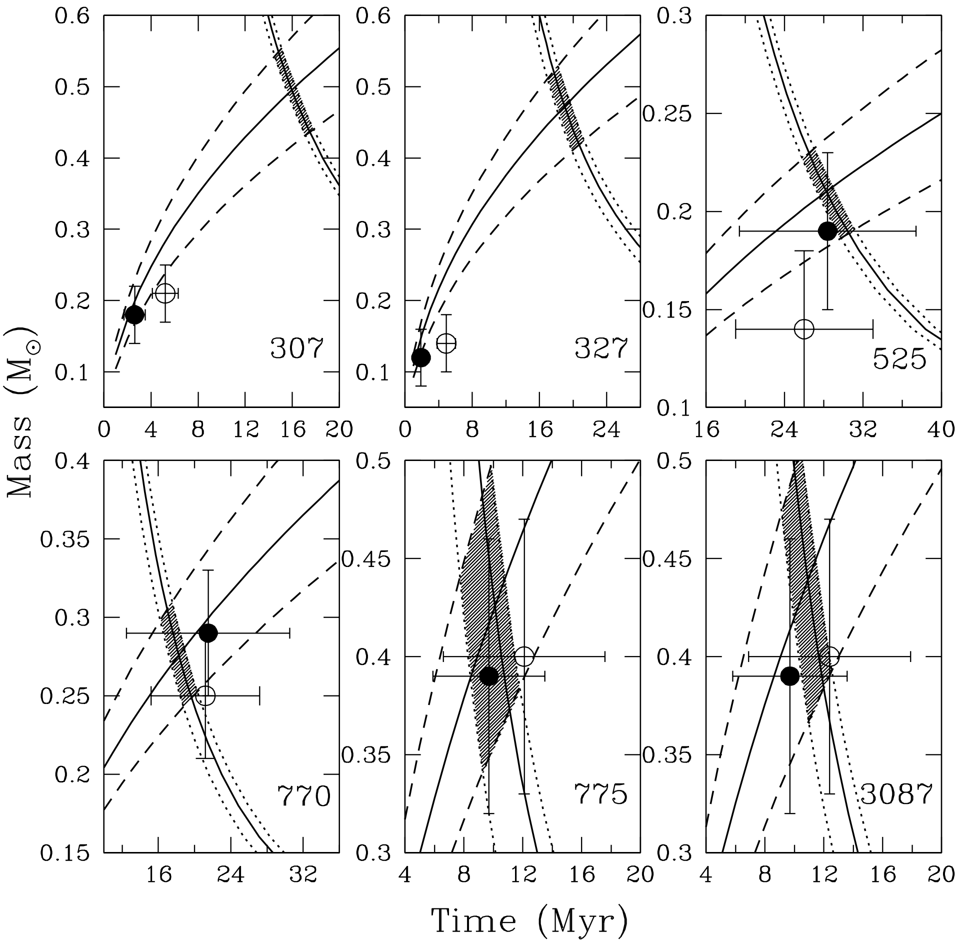

Fig. 3.— Mass vs. age plot for the six stars with evidence for Li depletion. For each star, we plot the luminosity curve (positive slope) and the Li abundance curve (negative slope) computed for the value of $T_{\rm eff}$ given in Table 1. The dashed curves give the uncertainty range in the observed L (± 0.2 dex, long-dash) and in the measured A(Li) (short-dash). The hatched region bounds the values of M and t consistent with the observations. In each panel, the solid points with errorbars give the mass and age from theoretical PMS tracks and isochrones (solid: PS99; empty: Siess et al. 2000).